JOURNAL OF SOLID STATE CHEMISTRY 107, 63–75 (1993)

Synthesis, Characterization, and Crystal Structure of Three Homoleptic Copper(I) Thiolates: $(Cu(CH_3S^-))_\infty$, $[(C_6H_5)_4P^+]_2[Cu_5(CH_3S^-)_7] \cdot C_2H_6O_2$, and $[(C_3H_7)_4N^+]_2[Cu_4(CH_3S^-)_6 \cdot CH_4O$

MARKUS BAUMGARTNER AND HELMUT SCHMALLE

Institute of Inorganic Chemistry, University of Zürich, Winterthurerstr. 190, CH-8057 Zürich, Switzerland

AND CHRISTIAN BAERLOCHER

Institute of Crystallography and Petrography, ETH-Zentrum, CH-8092 Zürich, Switzerland

Received October 8, 1992; in revised form February 22, 1993; accepted February 25, 1993

The structure of $(Cu(CH_3S^-))_x$ (I) has been solved, from X-ray powder diffraction data, in the space group $P4_2/m$ and with the unit cell $a = b = 8.4488(2)$ Å, $c = 4.0059(2)$ Å, $V = 285.9(1)$ Å^3, to residual factors $R = 7.3\%$ and $R_w = 12.5\%$. One soft restriction was used to restrain the C–S bond. The structure is built up of parallel chains, centred in 0, 0, Z, with the overall stoichiometry $Cu_x(CH_3S^-)_x$ and the symmetry S_4. The structures of $[(C_6H_5)_4P^+]_2[Cu_5(CH_3S^-)_7] \cdot C_2H_6O_2$ (II) and $[(C_3H_7)_4N^+]_2[Cu_4(CH_3S^-)_6] \cdot CH_4O$ (III) were solved from single crystal X-ray diffractometer data. Both compounds are triclinic. Compound (II) was refined in the space group $P\bar{1}$ with $a = 11.240(3)$ Å, $b = 13.066(3)$ Å, $c = 13.142(2)$ Å, $\alpha = 118.61(2)°$, $\beta = 92.48(2)°$, $\gamma = 111.85(2)°$, $V = 1514(2)$ Å^3, $Z = 1$. The structure contains molecular $[Cu_5(CH_3S^-)_7]^{2-}$ units, crystallized with the bulky $(C_6H_5)_4P^+$ cations. The lattice constants of compound (III) are $a = 12.125(2)$ Å, $b = 17.119(6)$ Å, $c = 24.256(5)$ Å, $\alpha = 105.54(2)°$, $\beta = 90.33(2)°$, $\gamma = 107.48(2)°$, $V = 4616(3)$ Å^3, space group $P\bar{1}$, $Z = 4$. The structure again is built up of molecular units: $[Cu_4(CH_3S^-)_6]^{2-}$ anions and bulky $(C_3H_7)_4N^+$ cations.

Introduction

The coordination chemistry of thiolates, a fundamental ligand type in transition metal chemistry (*1–3*) shows fascinating structural diversity not only for the polynuclear compounds but also for the polymeric aggregates. Many of these compounds represent substructures of metal sulfides, with the advantage that the substituent R of the ligating RS^- group can be manipulated to effect steric and electronic control of ligating ability and to engineer the environment around the metal site. Here we report an additional structural effect, the influence of bulky counterions favoring a specific metal–sulfur core type. An analogous observation was reported by Hartl about the crystallization of polynuclear Cu(I) iodides (*4*).

A large number of metal thiolates, particularly the uncharged compounds, are insoluble or slightly soluble in inert solvents and are therefore presumed to be structurally nonmolecular. Different techniques have been applied successfully to crystallize nonmolecular compounds, albeit insolubility makes it difficult to obtain crystals with a quality sufficient for diffraction analysis: (i) addition of noncoordinating solubilizing functions to the thiolate substituent R, (ii) a controlled slow shift of an equilibrium connecting the insoluble compound and a solu-

0022-4596/93 $5.00

ble (further ligated) species in solution, and (iii) a controlled thermal polymerization (*1*). We tried an additional preparative method: New phases can by synthesized by partial thermal decomposition. Different polynuclear Cu(I) thiolates, primarily investigated as model compounds for native Cu(I) thioneins (*5*), were used as precursors. The goal of this technique so far was the preparation of the uncharged Cu*R*S species ($R = CH_3$). Different structure types have been suggested for this compound, mostly based on IR data (*6–8*). The X-ray powder diffraction analysis performed by the Rietveld technique exhibits a new structure type for one-dimensionally nonmolecular metal thiolates.

Experimental

Synthesis

Materials and Methods. Sodium methane-thiolate (CH_3NaS), $(C_3H_7)_4NBr$, $(Ph)_4PBr$ and Cu_2O were purchased from Fluka AG, Buchs/Switzerland and used without further purification. The syntheses were performed in a Schlenk-type apparatus in nitrogen atmosphere.

Cu content and solvent molecules were determined by thermogravimetry (TG). The final product of these degradations was identified by X-ray powder diffraction analysis using a Guinier camera with a Johansson type monochromator ($CuK\alpha_1$ radiation). C, H and N analyses were performed by H. Frohofer, Institute of Organic Chemistry, University of Zürich.

Preparation of $(Cu(CH_3S^-))_\infty$ (*I*). This compound was obtained by thermal decomposition of $[(C_3H_7)_4N^+]_2[Cu_4(CH_3S^-)_6] \cdot CH_4O$ (III) as yellow needles. Anal. calc. for CH_3CuS: C 10.86%, H 2.73%, Cu 57.43%. Found: C 10.60%, H 2.71%, Cu 57.41%

Preparation of $[(C_6H_5)_4P^+]_2[Cu_5(CH_3S^-)_7] \cdot C_2H_6O_2$ (*II*). Cu_2O 310 mg (2.18 mmole) was added to a solution of 1.24 g (2.96 mmol) $(Ph)_4PBr$ and 200 mg (2.85 mmole) CH_3SNa in 12 ml of MeOH and 8 ml of ethylene glycol and 10 ml of CH_3CN. The solution was kept at 55°C for 1 hr until it became clear yellow. Then an additional 1.15 g (16.4 mmol) CH_3SNa was dissolved making the solution deep yellow. Slow evaporation at room temperature yielded orange-yellow crystals. Anal. calc. For $C_{57}H_{67}Cu_5O_2P_2S_7$: C 49.31%, H 4.86%, Cu 22.88%, solvent 4.47%. Found: C 48.81%, H 5.06%, Cu 23.14% (TG analysis), solvent 3.06% (TG analysis).

Preparation of $[(C_3H_7)_4N^+]_2[Cu_4(CH_3S^-)_6] \cdot CH_4O$ (*III*). Cu_2O 1.00 g (7.03 mmole) was added to a solution of 2.96 g (11.1 mmole) $(C_3H_7)_4NBr$ and 700 mg (9.98 mmole) CH_3SNa in 40 ml of MeOH and 25 ml of ethylene glycol and 25 ml of CH_3CN. This mixture was kept at 55°C for 1 hr until it became a clear pale yellow solution. Then an additional 2.27 g (32.36 mmol) CH_3SNa was dissolved making the solution yellowish. Slow evaporation at room temperature yielded colorless crystals. Anal. calc. for $C_{31}H_{78}Cu_4ON_2S_6$: C 39.55%, H 8.35%, Cu 26.99%, N 2.98%, solvent 3.40%. Found: C 39.47%, H 8.11%, Cu 26.65% (TG analysis), N 2.83%, solvent 3.50% (TG analysis).

Thermal Analysis

The thermal degradation of the compounds were registered on a Perkin Elmer TGS-2 thermobalance. The data in the temperature range of 30 to 500°C were recorded in flowing N_2 with a heating rate of 10°/min and 2.0–3.5 mg of sample. The gases evolved were simultaneously analysed with a Balzers QMG-511 quadrupole mass spectrometer coupled to the thermobalance (TG/MS).

High temperature-powder diffraction investigations were performed on a SIEMENS D 500 ($CuK\alpha$) with a high-temperature camera by ANTON PAAR KG (Graz, A). The experiments were run under inert atmosphere (N_2-flow 40 ml/min) and a heating rate of 10°/min. The interpretation of the raw data was done with the program DIFFRAC/AT.

Structure Determination

$(Cu(CH_3S^-))_\infty$ (*I*). The Guinier pattern was indexed with the program ITO (*9*) on a

tetragonal unit cell, and the lattice parameters refined to $a = b = 8.4488(2)$ Å and $c = 4.0059(2)$ Å. The observed systematic absences led to the space group $P4_2/m$ (or $P4_2$).

Comparison of the powder patterns obtained with a Guinier camera in transmission mode and with a diffractometer (flat plate) in reflection mode showed marked differences in peak intensities, indicating that the needle like crystals were preferentially oriented. To suppress this preferred orientation and to protect the material from the atmosphere, a sample was sealed in a 0.5 mm capillary. The powder pattern was then recorded with a Scintag PAD-X diffractometer on which a capillary rotating stage had been mounted. Such a modification of a Bragg-Brentano diffractometer has been described by Hill (*10*).

Diffracted intensities were measured every 0.02° 2θ in the range of 10 to 82° 2θ. Background values were estimated in areas of the pattern between peaks, linearly interpolated, and then subtracted from each data point. A "learned" standard peak shape function (*11*) was determined from the 110 peak at 14.78° 2θ. Further details pertaining to the data collection and the refinement are summarized in Table 1.

The X-ray Rietveld System XRS-82 (*12*) was used for the solution and refinement of the structure. The centrosymmetric space group $P4_2/m$ was assumed. Integrated intensities were extracted with the program EXTRACT (*13*) and the intensity of strongly overlapping reflections equipartitioned. The atomic positions of Cu and S could be deduced from a Patterson map generated from these data. With these atoms a Rietveld refinement was initiated and the CH_3 group located on a subsequent Fourier map. This position was then refined using the atomic scattering factor for C and a population parameter of 1.5. Attempts to include fixed hydrogen atoms did not improve the refinement. A geometric restraint of 1.835 Å had to be put on the C–S bond distance. A test refinement in the asymmetric space group did not show any significant differences in the structure. No absorption correction was applied.

The observed and calculated profiles are shown in Fig. 1. The final atomic parameters are given in Table II and selected bond distances and angles in Table III.

$[(C_6H_5)_4P^+]_2[Cu_5(CH_3S^-)_7] \cdot C_2H_6O_2$ (*II*) *and* $[(C_3H_7)_4N^+]_2[Cu_4(CH_3S^-)_6] \cdot CH_4O$ (*III*). Compound (II) was measured twice, as the assumption of space group $P\bar{1}$ proved to be wrong. $P\bar{1}$ refinement showed R and R_w values of about 20%. The second measurement collected 14724 intensity data (including 126 standards) of the whole limiting sphere. As the crystal size was relatively small, 8461 reflections had intensities $I < 3\sigma(I)$ and were considered unobserved ($\sigma(I)$ based on counting statistics). Thus 5628 reflections were used in the refinement, nine of them were omitted because secondary extinction was suspected. The atomic positions of the bulky $(C_6H_5)_4P^+$ cations were refined successfully not only in $P1$ ($Z = 1$, s.o.f. = 1) but also in $P\bar{1}$ ($Z = 1$, s.o.f. = 0.5). The Cu–S cluster did not refine well in the centrosymmetric space group $P\bar{1}$ because the center of symmetry generated split atomic positions with high displacement parameters u_{ij} for all the atoms of the cluster. To improve the precision of the atomic positions and to decrease the values of the displacement parameters, we finally refined the structure in $P1$ with two different oriented isomers for the $[Cu_5(CH_3S^-)_7]^{2-}$ anion cage, each of them with an s.o.f. of 0.5; the two isomers for the Cu-thiolate cluster can not be transformed accurately to each other by a centre of symmetry (see Table II). However, E-statistic (*14*) and $N(z)$ test (*15*), carried out with 7299 measured reflections (including unobserved; those with negative intensities were omitted), showed that the probability distribution of the data was between centric and hypercentric. Friedel pairs with large intensities were different with regard to the $2\sigma(I)$ criterion ($\sigma(I)$ based on counting statistics), referring to the noncentric part of the structure. Weissenberg photographs showed no indication of a superlattice.

TABLE I

EXPERIMENTAL DATA AND STRUCTURE REFINEMENT PARAMETERS FOR $(Cu(CH_3S^-))_x$ (I), $[(C_6H_5)_4P^+]_2[Cu_5(CH_3S^-)_7] \cdot C_2H_6O_2$ (III), AND $[(C_3H_7)_4N^+]_2[Cu_4(CH_3S^-)_6] \cdot CH_4O$ (III)

	(I)	(II)	(III)
Crystal shape and size	Powder (needles)	0.31 × 0.33 × 0.16 platelet	0.75 × 0.22 × 0.15 needles
Color	yellowish	orange-yellow	colorless
Lattice parameters (298 K)	$a = b = 8.4488(2)$ Å $c = 4.0059(2)$ Å $V = 285.9(1)$ Å^3	$a = 11.240(3)$ Å $b = 13.066(3)$ Å $c = 13.142(2)$ Å $\alpha = 118.61(2)°$ $\beta = 92.48(2)°$ $\gamma = 111.85(2)°$ $V = 1514(2)$ Å^3	$a = 12.125(2)$ Å $b = 17.119(6)$ Å $c = 24.256(5)$ Å $\alpha = 105.54(2)°$ $\beta = 90.33(2)°$ $\gamma = 107.48(2)°$ $V = 4616(3)$ Å^3
Space group	$P4_2/m$ (No. 84)	$P\bar{1}$	$P\bar{1}$
D_{calc}; Z	2.571; 4	1.523; 1	1.355; 4
Data collection technique	Powder, capillary	CAD-4 Enraf Nonius	CAD-4 Enraf Nonius
Scan mode	0.02°/step	ω–2Θ	ω–2Θ
Wavelength	Cu$K\alpha_1$	Mo$K\alpha$	Mo$K\alpha$
$(\sin\Theta/\lambda)_{max}$; Θ_{max}	0.462; 82.0°	0.66055; 28.0°	0.57228; 24.0°
No. of measured refl.	101	14,598	8760
hkl range	7, 7, 3	±14, ±17, ±17	−13/+2, −17/+19, −27/0
No. of refl. with $I > 3\sigma(I)$		5637	2832
No. of variables refined	9 + 8 (profile)	502	473
Absorption correction	none	based on 6 crystal faces	based on 8 crystal faces
Absorption coefficient	μ (Cu$K\alpha$) = 146.2 cm^{-1}	μ (Mo$K\alpha$) = 20.6 cm^{-1}	μ (Mo$K\alpha$) = 20.3 cm^{-1}
Extr. transmission factors		0.72, 0.53	0.78, 0.37
Atomic scattering factors f' and f''	neutral atoms	SHELX76 (*17*), International Table Vol IV (1974)	SHELX76 (*17*), International Table Vol IV (1974)
Weighting scheme	$1/\sigma^2$	unit weight ($w = 1$)	unit weight ($w = 1$)
R, R_w (%)	7.3, 12.5	8.7, 9.3	7.5, 8.6
$(\Delta/\sigma)_{max}$			0.114

In contrast, rotation and Weissenberg photographs of compound (III) showed superlattice reflections: Strong intensities are observed for hkl reflection with $l = 2n$ and only weak intensities for those with $l = 2n + 1$. The refinement was performed in space group $P\bar{1}$, $Z = 4$, using 2832 reflections; 16 of them were omitted because of secondary extinction.

Both structures (II) and (III) were solved using a combination of Patterson syntheses, conventional Fourier techniques and full-matrix least-squares refinements. The calculations were performed with the programs SHELXS86 (*16*) and SHELX76 (*17*). Due to a disordered arrangement of some of the terminal carbon atoms of the thiolate ligands, the S(x)-C(x) (x = any number) distance was treated with a constrained bond length (1.835(5) Å). In the final refinement copper, sulfur, phosphorus, nitrogen and the carbon atoms of the thiolate ligands in (II) were refined anisotropically and all other atoms with isotropic displacement factors. The phenyl-rings were included as rigid groups with free varying isotropic displacement factors. The carbon atoms and all the atoms of the inserted solvent molecules

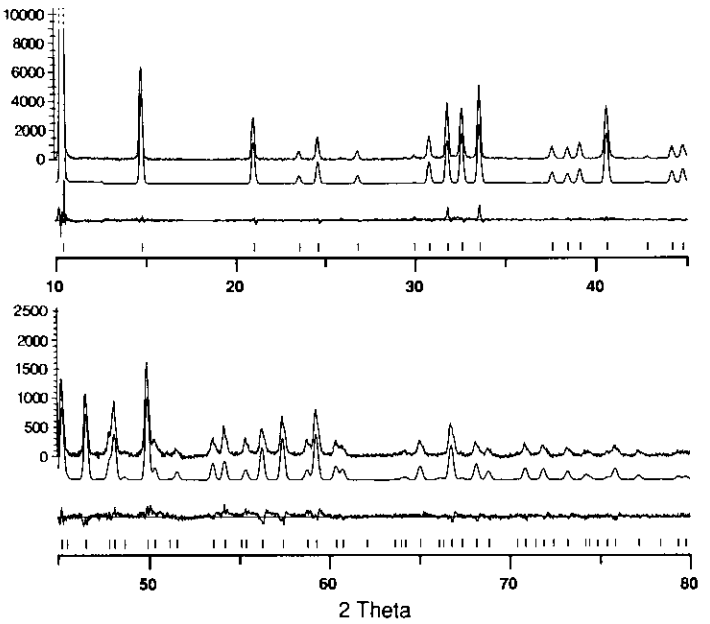

FIG. 1. Observed (top), calculated (middle), and difference (bottom) profiles for the Rietveld refinement of $(Cu(CH_3S^-))_\infty$ (I). The scale of the second part has been increased by a factor of 4 to show more detail.

were also treated with isotropic temperature factors. The position of the hydrogen atoms were calculated, and the H atoms were included as fixed contributions in the refinement. Experimental details of the data collection and the refinement are listed in Table I, final atomic parameters are given in Table II, selected bond length and angles in Table IV and V.

Bond distances and angles were calculated by the program ORFFE (*18*), stereoplots were generated by the program SCHAKAL (*19*).

Results and Discussion

Description of the Structures

Within the structure of $(Cu(CH_3S^-))_\infty$ (I), each copper atom is coordinated to three sulfur atoms in a trigonal planar manner; each of these thiolate sulfur atoms bridges three Cu(I) in a distorted tetrahedral $CSCu_3$ arrangement. These two elements are combined to form a polymeric chain structure with S_4 symmetry. In Fig. 2, a stereoview of the configuration of this structure is given. The chains running parallel to the *c*-axis are centered at 0, 0, *Z*. An additional structural feature is the six membered Cu_3S_3-ring often observed in polynuclear Cu(I) thiolates and Cu(I) sulfides.

This structure represents a new type of one-dimensionally nonmolecular metal thiolates and at the same time the second polymeric Cu(I) thiolate (*1, 20*). The similarity of the IR spectra of different polymeric $(Cu(RS^-))_\infty$ suggests that all these compounds might have similar structures (*6*).

Recently, two oligomeric complexes with a copper to sulfur ratio of 1 : 1 have been published: $[Cu_8(SC_6H_2(i\text{-}Pr)_3)_8]$ with a sixteen membered ring of alternating linear coordinated copper atoms and μ_2-S (*21*) and $[Cu_{12}(SC_6H_4(o\text{-}SiMe_3))_{12}]$ (*22, 23*). The second structure is best described as a $Cu_{12}S_{12}$ core arranged as a molecular paddle wheel: Two approximately parallel Cu_3S_3 rings are connected by three Cu atoms forming S_{ring}–Cu–S_{ring} bridges and three S–Cu–S

TABLE II: POSITIONAL PARAMETERS (Cu-, S- AND C-ATOMS OF THE Cu(I) THIOLATES, P- AND N-ATOMS OF THE CATIONS) OF $(Cu(CH_3S^-))_\infty$ (I), $[(C_6H_5)_4P^+]_2[Cu_5(CH_3S^-)_7] \cdot C_2H_6O_2$ (II) AND $[(C_3H_7)_4N^+]_2[Cu_4(CH_3S^-)_6] \cdot CH_4O$ (III)

	Atom	x	y	z	U_{eq}/U_{iso} (Å^2) a)
(I)	Cu	0.074(1)	0.172(1)	0.000	0.046(3)
	S	-0.196(2)	0.187(2)	0.000	0.023(6)
	C	-0.229(4)	0.402(2)	0.000	0.186(30)
(II)	Cu(1)	0.3435	0.3658	0.4581	0.0501(6)
	Cu(2)	0.4346(7)	0.6023(7)	0.6726(6)	0.0706(6)
	Cu(3)	0.5866(7)	0.5222(6)	0.4041(6)	0.0681(6)
	Cu(4)	0.5996(6)	0.4538(6)	0.5723(6)	0.0672(6)
	Cu(5)	0.5660(7)	0.7510(7)	0.5737(7)	0.0838(7)
	Cu(6)	0.6570(4)	0.6367(5)	0.5462(5)	0.0879(7)
	Cu(7)	0.5675(6)	0.3906(6)	0.3228(5)	0.0590(6)
	Cu(8)	0.4102(6)	0.4620(6)	0.5810(6)	0.0729(6)
	Cu(9)	0.4037(6)	0.5492(7)	0.4310(7)	0.0890(7)
	Cu(10)	0.4395(6)	0.2401(6)	0.4138(5)	0.0576(6)
	S(1)	0.2398(9)	0.4375(9)	0.5919(9)	0.0618(7)
	S(2)	0.4244(9)	0.7887(9)	0.6856(9)	0.0680(7)
	S(3)	0.6855(10)	0.7336(10)	0.4562(11)	0.0855(8)
	S(4)	0.4319(9)	0.2442(8)	0.4837(7)	0.0492(7)
	S(5)	0.7270(10)	0.4527(9)	0.4378(10)	0.0813(7)
	S(6)	0.3754(10)	0.3930(8)	0.3019(8)	0.0608(7)
	S(7)	0.6228(10)	0.6106(10)	0.7483(10)	0.0782(7)
	S(8)	0.7779(9)	0.5616(10)	0.4045(9)	0.0722(7)
	S(9)	0.5651(11)	0.2054(10)	0.3004(9)	0.0889(7)
	S(10)	0.3038(9)	0.2437(8)	0.5284(8)	0.0592(7)
	S(11)	0.5741(12)	0.7451(11)	0.4932(10)	0.1018(7)
	S(12)	0.2652(10)	0.5346(10)	0.5373(11)	0.0904(8)
	S(13)	0.6238(10)	0.5938(10)	0.6788(9)	0.0797(7)
	S(14)	0.3874(9)	0.3773(10)	0.2335(10)	0.0764(8)
	C(1)	0.1347(14)	0.4824(14)	0.5280(15)	0.0732(8)
	C(2)	0.5426(15)	0.9391(14)	0.8281(13)	0.0605(7)
	C(3)	0.6142(16)	0.7786(14)	0.3649(14)	0.0832(7)
	C(4)	0.3610(15)	0.2059(15)	0.5915(12)	0.0597(8)
	C(5)	0.8918(13)	0.5924(14)	0.5077(15)	0.0649(8)
	C(6)	0.2864(14)	0.4887(12)	0.3098(14)	0.0476(8)
	C(7)	0.7724(14)	0.7534(15)	0.7810(15)	0.0764(7)
	C(8)	0.8963(14)	0.5181(14)	0.4530(15)	0.0582(7)
	C(9)	0.4714(17)	0.1034(17)	0.1401(13)	0.1341(8)
	C(10)	0.3935(15)	0.2323(15)	0.6395(13)	0.0734(7)
	C(11)	0.6299(15)	0.7533(15)	0.3680(12)	0.0557(7)
	C(12)	0.1087(14)	0.3893(15)	0.4464(16)	0.0882(7)
	C(13)	0.6779(16)	0.4822(13)	0.6885(16)	0.1014(7)
	C(14)	0.2532(15)	0.2221(13)	0.1963(15)	0.0776(8)
	P(1)	0.0349(6)	0.2440(5)	0.8569(5)	0.0477(6)
	P(2)	-0.0303(6)	-0.2507(5)	0.1362(5)	0.0439(6)

	Atom	x	y	z	U_{eq}/U_{iso} (Å^2) a)
(III)	Cu(1)	0.3312(4)	0.2038(3)	0.1971(2)	0.058(1)
	Cu(2)	0.3917(4)	0.3393(3)	0.1534(2)	0.051(1)
	Cu(3)	0.1673(3)	0.2675(2)	0.1752(2)	0.049(1)
	Cu(4)	0.2680(4)	0.1893(3)	0.0826(2)	0.066(1)
	Cu(5)	-0.0330(4)	0.3365(3)	0.6549(2)	0.065(2)
	Cu(6)	0.1303(3)	0.2602(2)	0.6739(2)	0.046(1)
	Cu(7)	-0.0842(4)	0.2015(3)	0.6986(2)	0.060(1)
	Cu(8)	-0.0423(4)	0.1861(3)	0.5850(2)	0.056(1)
	S(1)	0.5017(7)	0.3119(5)	0.2168(5)	0.060(3)
	S(2)	0.1789(9)	0.2144(5)	0.2500(4)	0.064(3)
	S(3)	0.3008(8)	0.0874(5)	0.1194(5)	0.064(3)
	S(4)	0.2561(8)	0.4076(5)	0.1812(5)	0.060(3)
	S(5)	0.3997(9)	0.2933(6)	0.0577(5)	0.072(4)
	S(6)	0.0753(7)	0.1871(5)	0.0878(4)	0.048(3)
	S(7)	0.1622(7)	0.4018(5)	0.6803(4)	0.057(3)
	S(8)	-0.1608(8)	0.3101(6)	0.7174(5)	0.061(3)
	S(9)	-0.0789(8)	0.2946(6)	0.5570(5)	0.069(3)
	S(10)	0.0789(8)	0.2093(5)	0.7503(4)	0.040(3)
	S(11)	0.1489(8)	0.1834(6)	0.5827(5)	0.086(4)
	S(12)	-0.1635(7)	0.0874(5)	0.6213(4)	0.051(3)
	C(1)	0.4909(27)	0.3856(18)	0.2852(9)	0.057(9)
	C(2)	0.0862(27)	0.1030(12)	0.2288(16)	0.060(9)
	C(3)	0.4439(19)	0.0793(24)	0.0992(16)	0.086(12)
	C(4)	0.2159(33)	0.4189(22)	0.1110(11)	0.070(10)
	C(5)	0.5331(23)	0.2647(26)	0.0450(17)	0.098(14)
	C(6)	0.0030(25)	0.0747(11)	0.0817(15)	0.048(8)
	C(7)	0.2138(24)	0.4139(20)	0.6119(9)	0.060(9)
	C(8)	-0.0865(40)	0.3855(20)	0.7854(13)	0.098(14)
	C(9)	-0.2370(14)	0.2682(23)	0.5465(18)	0.076(11)
	C(10)	0.0845(30)	0.0998(12)	0.7303(15)	0.061(9)
	C(11)	0.1320(33)	0.0701(11)	0.5716(18)	0.069(10)
	C(12)	-0.3065(19)	0.0936(26)	0.6082(20)	0.092(13)
	N(1)	0.0455(19)	-0.1981(13)	0.0815(9)	0.067(9)
	N(2)	-0.1318(17)	0.3261(12)	0.2603(11)	0.073(11)
	N(3)	0.5231(17)	0.6790(15)	0.2393(10)	0.066(9)
	N(4)	0.2841(17)	0.2002(13)	0.4180(11)	0.038(9)

a) $U_{eq} = \frac{1}{3} \sum_i \sum_j U_{ij} a_i^* a_j^* \mathbf{a}_i \mathbf{a}_j$.

TABLE III

SELECTED BOND DISTANCES (Å), ANGLES (°) AND THE DEVIATION (Å) OF THE Cu ATOM FROM THE CORRESPONDING S_3-PLANES FOUND IN (I).

Bond distances (Å)		Angles (°)	
Cu–S	2.284(19)	S–Cu–S(i, ii)	115.0(4)
Cu–S(i, ii)	2.229(7)	S(i)–Cu–S(ii)	128.1(9)
Cu–Cu(i, ii, iii, iv)	3.003(9)	Cu(iii)–S–Cu(iv)	128.1(9)
Cu–Cu(v, vi)	4.006(1)	Cu–S–Cu(iii, iv)	83.4(6)
Deviation	0.180	Cu–S–C	101.9(1.3)
S–C	1.837(24)	Cu(iii, iv)–S–C	115.9(4)

Sym. op: *(i)*, $y, -x, \frac{1}{2} + z$; *(ii)*, $y, -x, -\frac{1}{2} + z$; *(iii)*, $-y, x, \frac{1}{2} + z$; *(iv)*, $-y, x, \frac{1}{2} + z$; (v), $x, y, 1 + z$; (vi), $x, y, -1 + z$.

TABLE IV

S–Cu–S COORDINATION ANGLES (°), DEVIATION (Å) OF THE Cu ATOMS FROM THE CORRESPONDING S_3-PLANES AND Cu–S BOND DISTANCES (Å, IN ORDER OF INCREASING S-LABEL) FOUND IN (II) AND (III)

(II)	(°)	(Å)	Cu-S (Å)		(°)	(Å)	Cu-S (Å)
S(1)-Cu(1)-S(4)	113.1(4)		2.177(11)	S(8)-Cu(6)-S(11)	95.8(6)		2.117(17)
S(1)-Cu(1)-S(6)	130.0(5)	0.001	2.298(12)	S(8)-Cu(6)-S(13)	130.8(6)	0.059	2.396(12)
S(4)-Cu(1)-S(6)	116.9(4)		2.267(12)	S(11)-Cu(6)-S(13)	132.9(6)		2.288(20)
S(1)-Cu(2)-S(2)	110.9(6)		2.158(10)	S(8)-Cu(7)-S(9)	112.9(5)		2.299(9)
S(1)-Cu(2)-S(7)	126.3(7)	0.048	2.405(16)	S(8)-Cu(7)-S(14)	126.9(6)	0.155	2.283(17)
S(2)-Cu(2)-S(7)	122.6(4)		2.241(16)	S(9)-Cu(7)-S(14)	118.7(4)		2.200(15)
S(3)-Cu(3)-S(5)	114.1(5)		2.274(15)	S(10)-Cu(8)-S(13)	123.6(6)		2.355(13)
S(3)-Cu(3)-S(6)	121.5(6)	0.112	2.215(17)	S(12)-Cu(8)-S(13)	122.4(6)	0.067	2.340(18)
S(5)-Cu(3)-S(6)	123.7(5)		2.204(11)	S(10)-Cu(8)-S(12)	113.7(4)		2.218(11)
S(4)-Cu(4)-S(5)	106.8(4)		2.308(9)	S(11)-Cu(9)-S(12)	119.7(5)		2.153(15)
S(4)-Cu(4)-S(7)	123.1(5)	0.009	2.320(15)	S(11)-Cu(9)-S(14)	113.3(5)	0.071	2.258(13)
S(5)-Cu(4)-S(7)	130.0(5)		2.151(12)	S(12)-Cu(9)-S(14)	126.8(4)		2.427(12)
S(2)-Cu(5)-S(3)	168.9(8)		2.243(14)	S(9)-Cu(10)-S(10)	169.8(7)		2.106(14)
			2.077(15)				2.186(13)
(III)	(°)	(Å)	(Å)		(°)	(Å)	(Å)
S(1)-Cu(1)-S(2)	120.6(4)		2.270(8)	S(7)-Cu(5)-S(8)	123.5(4)		2.296(9)
S(1)-Cu(1)-S(3)	121.4(4)	0.065	2.283(12)	S(7)-Cu(5)-S(9)	112.5(4)	0.040	2.211(12)
S(2)-Cu(1)-S(3)	117.8(3)		2.278(10)	S(8)-Cu(5)-S(9)	123.8(4)		2.301(12)
S(1)-Cu(2)-S(4)	122.6(4)		2.260(12)	S(7)-Cu(6)-S(10)	121.0(4)		2.298(10)
S(1)-Cu(2)-S(5)	121.9(5)	0.046	2.300(11)	S(7)-Cu(6)-S(11)	111.8(5)	0.033	2.266(11)
S(4)-Cu(2)-S(5)	115.4(5)		2.256(13)	S(10)-Cu(6)-S(11)	127.2(4)		2.302(13)
S(2)-Cu(3)-S(4)	121.8(4)		2.256(13)	S(8)-Cu(7)-S(10)	121.9(4)		2.263(12)
S(2)-Cu(3)-S(6)	123.7(4)	0.031	2.279(9)	S(8)-Cu(7)-S(12)	118.3(4)	0.062	2.289(11)
S(4)-Cu(3)-S(6)	114.5(4)		2.263(9)	S(10)-Cu(7)-S(12)	119.6(4)		2.270(9)
S(3)-Cu(4)-S(6)	110.7(4)		2.290(13)	S(9)-Cu(8)-S(11)	116.0(4)		2.297(13)
S(5)-Cu(4)-S(6)	121.2(5)	0.111	2.230(12)	S(9)-Cu(8)-S(12)	128.5(4)	0.059	2.339(12)
S(3)-Cu(4)-S(5)	127.3(4)		2.335(10)	S(11)-Cu(8)-S(12)	115.3(5)		2.262(11)

TABLE V

STEREOCHEMISTRY OF THE μ_2-BRIDGING THIOLATES (°, Å) AND Cu–Cu DISTANCES (Å) FOUND IN (II) AND (III)

(II)	Cu-S-Cu (°)	Cu-Cu (Å)		Cu-S-C (°)	S-C (Å)
Cu(1)-S(1)-Cu(2)	79.1(4)	2.756(6)	Cu(1)-S(1)-C(1)	105.3(8)	1.829(26)
			Cu(2)-S(1)-C(1)	105.3(8)	
Cu(2)-S(2)-Cu(5)	75.4(5)	2.845(13)	Cu(2)-S(2)-C(2)	109.5(9)	1.858(13)
			Cu(5)-S(2)-C(2)	100.3(7)	
Cu(3)-S(3)-Cu(5)	81.8(5)	2.853(11)	Cu(3)-S(3)-C(3)	118.1(6)	1.836(28)
			Cu(5)-S(3)-C(3)	99.1(9)	
Cu(1)-S(4)-Cu(4)	72.3(4)	2.715(7)	Cu(1)-S(4)-C(4)	108.0(8)	1.836(21)
			Cu(4)-S(4)-C(4)	113.9(5)	
Cu(3)-S(5)-Cu(4)	75.2(5)	2.769(13)	Cu(3)-S(5)-C(5)	106.3(9)	1.827(14)
			Cu(4)-S(5)-C(5)	113.3(7)	
Cu(1)-S(6)-Cu(3)	87.4(4)	3.090(7)	Cu(1)-S(6)-C(6)	103.3(8)	1.841(23)
			Cu(3)-S(6)-C(6)	110.8(6)	
Cu(2)-S(7)-Cu(4)	88.4(5)	3.063(12)	Cu(2)-S(7)-C(7)	113.5(10)	1.824(18)
			Cu(4)-S(7)-C(7)	106.7(8)	
Cu(6)-S(8)-Cu(7)	75.5(4)	2.875(7)	Cu(6)-S(8)-C(8)	114.5(9)	1.827(25)
			Cu(7)-S(8)-C(8)	110.0(8)	
Cu(7)-S(9)-Cu(10)	78.1(5)	2.769(11)	Cu(7)-S(9)-C(9)	93.6(10)	1.844(17)
			Cu(10)-S(9)-C(9)	111.7(8)	
Cu(8)-S(10)-Cu(10)	77.0(4)	2.831(10)	Cu(8)-S(10)-C(10)	107.0(6)	1.833(25)
			Cu(10)-S(10)-C(10)	99.4(8)	
Cu(6)-S(11)-Cu(9)	72.7(6)	2.693(9)	Cu(6)-S(11)-C(11)	111.4(10)	1.822(23)
			Cu(9)-S(11)-C(11)	112.1(6)	
Cu(8)-S(12)-Cu(9)	74.3(5)	2.718(15)	Cu(8)-S(12)-C(12)	105.7(10)	1.825(14)
			Cu(9)-S(12)-C(12)	111.3(8)	
Cu(6)-S(13)-Cu(8)	91.7(5)	3.084(9)	Cu(6)-S(13)-C(13)	120.7(9)	1.827(26)
			Cu(8)-S(13)-C(13)	101.0(7)	
Cu(7)-S(14)-Cu(9)	85.8(4)	3.155(11)	Cu(7)-S(14)-C(14)	105.2(10)	1.827(18)
			Cu(9)-S(14)-C(14)	109.5(8)	

(III)	Cu-S-Cu (°)	Cu-Cu (Å)		Cu-S-C (°)	S-C (Å)
Cu(1)-S(1)-Cu(2)	73.5(3)	2.710(7)	Cu(1)-S(1)-C(1)	106.0(10)	1.828(25)
			Cu(2)-S(1)-C(1)	103.1(12)	
Cu(1)-S(2)-Cu(3)	71.6(4)	2.654(7)	Cu(1)-S(2)-C(2)	100.6(12)	1.830(20)
			Cu(3)-S(2)-C(2)	107.3(13)	
Cu(1)-S(3)-Cu(4)	75.7(3)	2.802(8)	Cu(1)-S(3)-C(3)	107.6(10)	1.845(29)
			Cu(4)-S(3)-C(3)	106.8(15)	
Cu(2)-S(4)-Cu(3)	74.0(3)	2.754(6)	Cu(2)-S(4)-C(4)	98.6(13)	1.845(34)
			Cu(3)-S(4)-C(4)	104.8(11)	
Cu(2)-S(5)-Cu(4)	72.8(4)	2.663(5)	Cu(2)-S(5)-C(5)	108.5(14)	1.833(36)
			Cu(4)-S(5)-C(5)	109.4(15)	
Cu(3)-S(6)-Cu(4)	74.5(3)	2.783(7)	Cu(3)-S(6)-C(6)	115.5(13)	1.824(21)
			Cu(4)-S(6)-C(6)	101.0(11)	
Cu(5)-S(7)-Cu(6)	74.4(3)	2.778(7)	Cu(5)-S(7)-C(7)	101.3(9)	1.821(27)
			Cu(6)-S(7)-C(7)	104.9(11)	
Cu(5)-S(8)-Cu(7)	74.3(4)	2.703(8)	Cu(5)-S(8)-C(8)	103.2(13)	1.828(30)
			Cu(7)-S(8)-C(8)	106.8(16)	
Cu(5)-S(9)-Cu(8)	70.3(4)	2.646(6)	Cu(5)-S(9)-C(9)	105.8(14)	1.836(20)
			Cu(8)-S(9)-C(9)	107.0(14)	
Cu(6)-S(10)-Cu(7)	70.6(3)	2.632(6)	Cu(6)-S(10)-C(10)	106.5(12)	1.827(25)
			Cu(7)-S(10)-C(10)	104.4(12)	
Cu(6)-S(11)-Cu(8)	72.6(4)	2.746(6)	Cu(6)-S(11)-C(11)	116.9(15)	1.832(24)
			Cu(8)-S(11)-C(11)	102.8(13)	
Cu(7)-S(12)-Cu(8)	75.1(3)	2.763(8)	Cu(7)-S(12)-C(12)	103.2(13)	1.829(32)
			Cu(8)-S(12)-C(12)	105.8(16)	

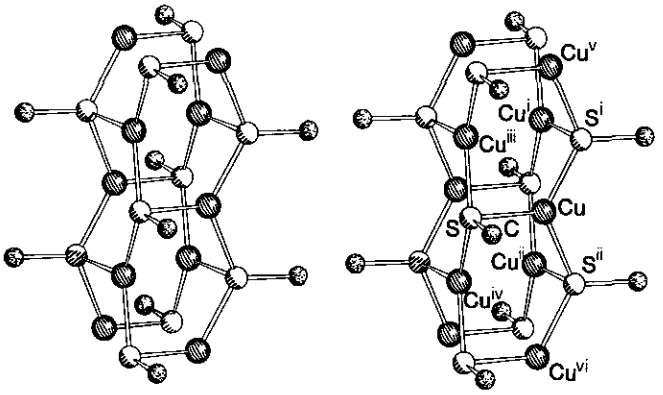

FIG. 2. Stereoplot of the $(Cu(CH_3S^-))_x$ chain in (I) with numbering scheme. The indices correspond with the symmetry operators given in Table III.

units are linking the Cu_{ring} atoms. Compared to (I) these structure types exhibit no related structural elements beside the Cu_3S_3 rings in the second one. However, the Cu–S framework in $[Cu_8(SC_5H_{11})_4(S_2CSC_5H_{11})_4]$ represents a real substructure of the polymeric chain structure found in (I) (*24, 25*). This molecular compound is formed by an insertion of CS_2 in $Cu_n(SC_5H_{11})_n$. Because the reaction presumably takes place at the boundaries of the oligomer, it is obvious that the structure retains some of the features of the unit (*25*).

In (I), metal–metal distances between two μ_3-S bridged Cu atoms are 3.003(9) Å or 4.007(1) Å, corresponding to the Cu–(μ_3-S)–Cu angles of 83.4(6)° and 128.1(9)°, respectively. The Cu–S distances range from 2.23(1) Å to 2.28(2) Å. All these values are comparable to those found in Cu(I) thiolate structures containing μ_3-thiolate ligands (*5, 20, 22–28*). The copper atom in (I) is displaced 0.180 Å from the plane through the three S atoms toward the center of the chain. This deviation is caused by geometrical restriction more than by the possibility of Cu–Cu bonding. The shortest interchain Cu–Cu distance is 3.16(2) Å. The S–C distance was restrained to 1.835(5) Å. This value is the average taken from ten Cu(I) thiolate structures, investigated by X-ray analysis (*5*) and corresponds to the mean value of 1.838(40) Å found in $[(CH_3)_4N]_2[Cu_4(CH_3S^-)_6]$ (*29*). Selected bond distances and angles are summarized in Table III.

The two compounds $[(C_6H_5)_4P^+]_2[Cu_5(CH_3S^-)_7] \cdot C_2H_6O_2$ (II) and $[(C_3H_7)_4N^+]_2[Cu_4(CH_3S^-)_6] \cdot CH_4O$ (III) exhibit both molecular anionic $[Cu_xRS_y]^{2-}$ units, separated by bulky cations. The refinements of these cations $(C_6H_5)_4P^+$ and $(C_3H_7)_4N^+$ show no unexpected geometries. Thus, lists of atomic positions and relevant bond distances and angles of these ordinary cations are deposited with the supplementary material.[1]

The structure of (III) consists of $[(Cu_4S_6)^{2-}]$ adamantane-type cluster units, separated by the $[(C_3H_7)_4N^+]$ cations. The structure of the cluster anion can be considered as a tetrahedron of copper atoms inscribed in a distorted octahedron of six μ_2-sulfur atoms (Fig. 3). This cluster type is the most common for Cu(I)-thiolates (*5, 18, 29–34*). The Cu–Cu distances range from 2.632(6) to 2.802(8) Å with a mean distance of 2.720 Å, the Cu–S distances from 2.211(12) to 2.339(10) Å, with a mean distance of 2.279 Å,and the Cu–S–Cu angles

[1] Additional material to this paper can be ordered from the Fachinformationszentrum Karlsruhe, 76344 Eggenstein-Leopoldshafen 2, Federal Republic of Germany. Please quote reference No. CSD-56668, the names of authors, and the title of the paper.

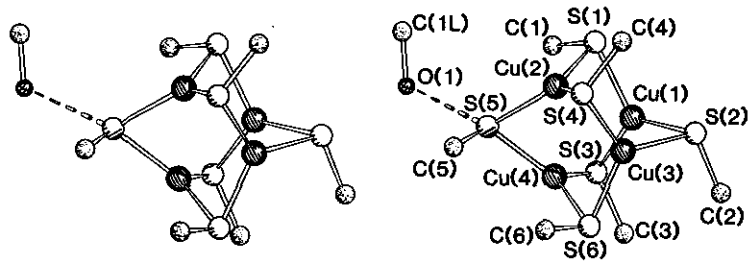

FIG. 3. Stereoplot of the adamantane-type $[Cu_4(CH_3S^-)_6]^{2-}$ cluster anion in $[(C_3H_7)_4N^+]_2[Cu_4(CH_3S^-)_6] \cdot CH_4O$ (III) with numbering scheme.

range from 70.3(4)° to 75.7(3)°. All copper atoms in (III) are systematically displaced from the plane through the three S atoms away from the centroid of the cage. These results are in agreement with data obtained in a similar structure: $[(CH_3)_4N^+]_2[Cu_4(CH_3S^-)_6]$ (*29*).

Different cations can favor the formation of different clusters, but no distinction is evident for $(CH_3)_4N^+$ and $(C_3H_7)_4N^+$. The structurally rigid $(C_6H_5)_4P^+$ group allows the enlarged adamantane-type unit, the $(Cu_5S_7)^{2-}$ core type to form. A reverse influence of the cations $(CH_3)_4N^+$ and $(C_6H_5)_4P^+$ is observed for Cu(I) thiolates with the thiophenolate ligand (*30*). The structure of $[(C_6H_5)_4P^+]_2[Cu_5(CH_3S^-)_7] \cdot C_2H_6O_2$ (II) is therefore the second example containing this $(Cu_5S_7)^{2-}$ core type (*30, 35, 36*). This polyhedron may be regarded as a structural derivation of the $(Cu_4S_6)^{2-}$ cluster obtained by opening two of the trigonal coordination planes of the S_6 octahedron and replacing the linking sulfur atom by a linear S–Cu–S group. Thus, the unit contains four trigonally and one linearly coordinated copper atom (see Fig. 4). The following mean values for bond distances and angles have been determined (a full list is given in Table V): Cu–Cu 2.873 Å (μ_2-S bridged), Cu_{trig}–S 2.265 Å, Cu_{dig}–S 2.153 Å. The S–C distance was again restrained to 1.835(5) Å.

The solvate molecules within the units in both structures are linked with the Cu–S cluster by hydrogen bonds of the type S · · · H–O. The corresponding S · · · O acceptor-donor distances in (II) are between 3.01(2) and 3.35(2) Å, mean 3.22 Å, and in (III) 3.21(4) and 3.15(4) Å, mean 3.18 Å. Similar ranges are discussed in other structures with solvate molecules linked to metal coordinating thiolates (*5, 20, 37–40*). The ethylene glycol molecule in (II) is connected with both OH groups to the $(Cu_5S_7)^{2-}$ core and thus forms a seven membered ring (see Fig. 4).

Thermogravimetry

The compounds were investigated by thermogravimetry (TG) because of different reasons: In order to determine the stoichiometries the inserted solvent molecules and the metal content have been quantified. An additional point was the elucidation of decomposition pathways and, as a final consequence of these investigations, to elaborate preparative methods to obtain special phases.

The thermogravimetric decomposition of the two compounds (II) and (III), built up by molecular units, exhibit a prestep where the inserted solvent molecules are removed. This desolventization is not clearly resolved in the case of (III). The identification of the inserted solvents was performed by mass-spectrometry.

The course of the subsequent degradations indicates the following characteristics: Compound (II) is decomposed in one broad step. On the other hand, a two step pathway is observed in the case of (III), where the first of these steps is again divided into two

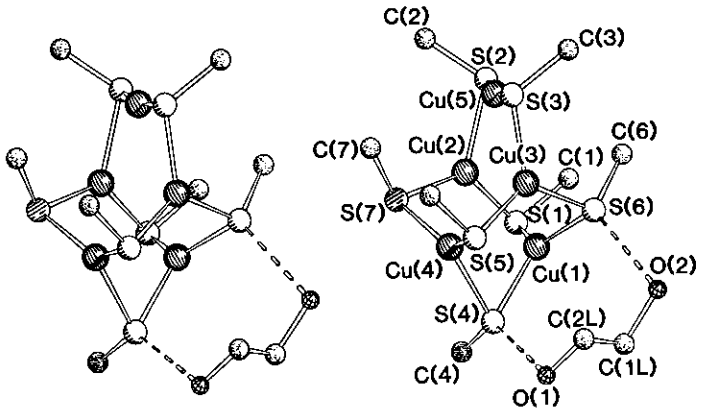

FIG. 4. Stereoplot of the $[Cu_5(CH_3S^-)_7]^{2-}$ cluster anion (with numbering scheme) in $[(C_6H_5)_4P^+]_2[Cu_5(CH_3S^-)_7] \cdot C_2H_6O_2$ (II).

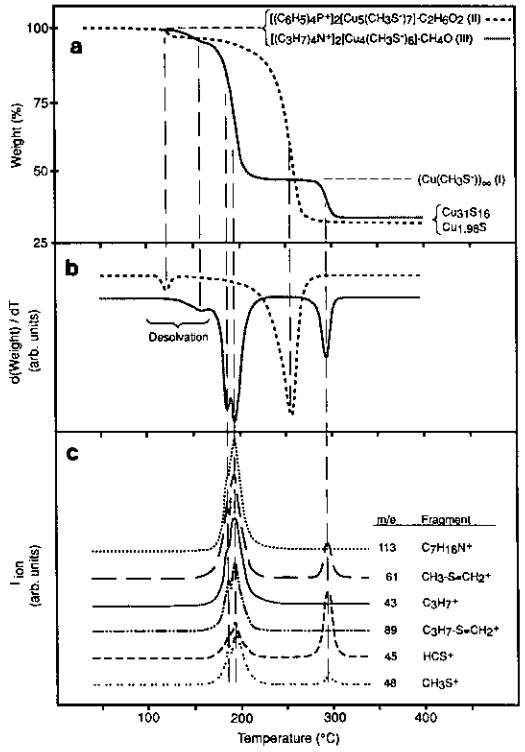

FIG. 5. (a) Thermal degradation of $[(C_6H_5)_4P^+]_2[Cu_5(CH_3S^-)_7] \cdot C_2H_6O_2$ (II) and $[(C_3H_7)_4N^+]_2[Cu_4(CH_3S^-)_6] \cdot CH_4O$ (III), (b) First derivative of this decrease of weight as a function of temperature, and (c) the simultaneously registered masses of evolved gas molecules during the decomposition of (III).

sections. Figure 5 shows the decrease of weight of the compounds while heating the samples, the first derivative of this function and, in the case of (III) only, the courses of the simultaneously registered masses of evolved gas molecules. An analysis and interpretation of these features is discussed in detail elsewhere (*41*).

$(Cu(CH_3S^-))_\infty$ (I) is a stable intermediate in the temperature range 210–280°C during the decomposition of (III). It is obtained as thin needles crystallized in a melt of (III). Variation of the heat rate or the sample amount has no influence nor on the size nor on the shape of the crystals. Investigations of other compounds exhibiting a stable intermediate of the stoichiometry $Cu_x(RS^-)_x$ during the thermal decomposition have not yet been obtained in crystalline form. We assume this to be a consequence of the low melting point of 153°C of (III) (*5, 41*).

The final product of these degradations is a mixture of different Cu(I) sulfides. Figure 6 shows the temperature profile of the combined heating-X-ray diffraction investigations and the corresponding phases. At 500°C only one high-temperature phase Cu_2S (ASTM No. 12-176 (*42*)) was observed, together with monoclinic Chalcocite (ASTM Nos. 23-961 and 33-490). While cooling to 150°C and then to room temperature (RT), the formation of two new phases,

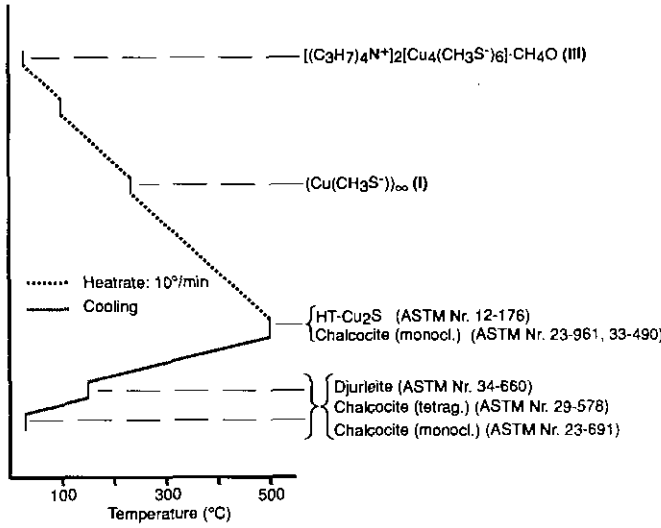

FIG. 6. The temperature profile of the combined high temperature-X-ray diffraction investigations of $[(C_3H_7)_4N^+]_2[Cu_4(CH_3S^-)_6] \cdot CH_4O$ (III) and the observed phases identified by the ASTM card index (*42*).

Djurleite (ASTM No. 34-660) and tetragonal Chalcocite (ASTM No. 29-578), is observed. In addition a very small amount of monoclinic Chalcocite (ASTM No. 23-961) is observed. So far, the formation of Djurleite is observed as final product only within the decomposition of $[(C_3H_7)_4N^+]_2[Cu_4(CH_3S^-)_6] \cdot CH_4O$ (III). This behavior is remarkable with respect to the fact that tetragonal chalcocite is metastable and converts to djurleite with time at RT (*43–46*). The relationship between these two phases is still not well understood. Annealing at temperatures above 100°C, slightly cooling to RT or syntheses under high pressure favors the formation of the metastable chalcocite phase (*45–47*). On the other hand, djurleite is more easily synthesized at a slight copper deficiency (*44*). Thus the composition of the final product of the thermal decomposition of the compounds under investigation seems to be contingent with respect to all the different Cu(I)–S cluster types, thiolate ligands and cations. To determine the metal content of the compounds, the stoichiometry of the predominant phase was used.

Acknowledgments

We thank Professor H. R. Oswald for supporting this project. Research grants from the Swiss national Science Foundation are gratefully acknowledged.

References

1. I. G. DANCE, *Polyhedron* **5,** 1037 (1986).
2. P. J. BLOWER AND J. R. DILWORTH, *Coord. Chem. Rev.* **76,** 121 (1987).
3. B. KREBS AND G. HENKEL, *Angew. Chem.* **103,** 785 (1991).
4. G. HERRSCHAFT AND H. HARTL, *Z. Kristallogr.* **178,** 95 (1987).
5. M. BAUMGARTNER, Ph.D. thesis, University of Zürich (1990).
6. G. A. BOWMAKER AND L.-C. TAN, *Aust. J. Chem.* **32,** 1443 (1979).
7. A. J. CANTY, R. KISHIMOTO, G. B. DEACON, AND G. J. FARQUHARSON, *Inorg. Chim. Acta* **20,** 161 (1976).
8. R. K. CHADHA, R. KUMAR, AND D. G. TUCK, *Can. J. Chem.* **65,** 1336 (1987).
9. J. W. VISSER, *J. Appl. Crystallogr.* **2,** 89 (1969).
10. R. J. HILL AND I. C. MADSEN, *Z. Kristallogr.* **196,** 73 (1991).
11. A. HEPP AND CH. BAERLOCHER, *Aust. J. Phys.* **41,** 229 (1988).
12. CH. BAERLOCHER, "XRS-82. The X-Ray Rietveld System XRS-82," Institut für Kristallographie, ETH, Zürich (1982).
13. CH. BAERLOCHER, "EXTRACT, A Fortran Program for the Extraction of Integrated Intensities from a Powder Pattern," Institut für Kristallographie, ETH, Zürich (1990).
14. I. L. KARLE, K. S. DRAGONETTE, AND S. A. BRENNER, *Acta Crystallogr.* **19,** 713 (1965).
15. E. R. HOWELLS, D. C. PHILLIPS, AND D. ROGERS, *Acta Crystallogr.* **3,** 210 (1950).
16. G. M. SHELDRICK, SHELXS-86, *in* "Crystallographic Computing," (G. M. Sheldrick, C. Krüger,

and R. Goddard, Eds.), p. 175, Oxford Univ. Press, Oxford (1985).
17. G. M. SHELDRICK, "SHELX-76, Program for Crystal Structure Determination," University of Cambridge, Cambridge (1976).
18. W. R. BUSING, K. O. MARTIN, H. A. LEVY, G. M. BROWN, C. K. JOHNSON, AND W. A. THIESSEN, "ORFFE3. A Fortran Function and Error Program," Oak Ridge National Laboratory, Oak Ridge, TN (1971).
19. E. KELLER, "SCHAKAL86, A Fortran Program for the Graphic Representation of Molecular and Crystallographic Models," University of Freiburg (1986).
20. M. BAUMGARTNER, H. SCHMALLE, AND E. DUBLER, *Polyhedron* **9,** 1155 (1990).
21. Q. YANG, K. TANG, H. LIAO, Y. HAN, Z. CHEN, AND Y. TANG, *J. Chem. Soc. Chem. Commun.* 1076 (1987).
22. E. BLOCK, M. GERNON, HYUNKYU KANG, SCHUNCHENG LIU, AND J. ZUBIETA, *J. Chem. Soc. Chem. Commun.* 1031 (1988).
23. E. BLOCK, M. GERNON, HYUNKYU KANG, G. OFORI-OKAI, AND J. ZUBIETA, *Inorg. Chem.* **28,** 1263 (1989).
24. R. K. CHADHA, R. KUMAR, AND D. G. TUCK, *J. Chem. Soc. Chem. Commun.* 188 (1986).
25. R. K. CHADHA, R. KUMAR, AND D. G. TUCK, *Polyhedron* **7,** 1121 (1988).
26. I. G. DANCE, G. A. BOWMAKER, G. R. CLARK, AND J. K. SEADON, *Polyhedron* **2,** 1031 (1983).
27. G. HENKEL, P. BETZ, AND B. KREBS, "XXIV Int. Conference on Coord. Chem., Athens, Greece," Abstr. Book, p. 737 (1986).
28. T. A. ANNAN, R. KUMAR, AND D. G. TUCK, *Inorg. Chem.* **29,** 2475 (1990).
29. I. G. DANCE, M. L. SCUDDER, AND L. J. FITZPATRICK, *Inorg. Chem.* **24,** 2547 (1985).
30. M. BAUMGARTNER, W. BENSCH, P. HUG, AND E. DUBLER, *Inorg. Chim. Acta* **136,** 139 (1987).
31. G. HENKEL, B. KREBS, P. BETZ, H. FIETZ, AND K. SAATKAMP, *Angew. Chem.* **100,** 1373 (1988).
32. D. COUCOUVANIS, C. N. MURPHY, AND S. K. KANODIA, *Inorg. Chem.* **19,** 2993 (1980).
33. I. G. DANCE AND J. C. CALABRESE, *Inorg. Chim. Acta* **19,** 141 (1976).
34. J. R. NICHOLSON, I. L. ABRAHAMS, W. CLEGG, AND C. D. GARNER, *Inorg. Chem.* **24,** 1092 (1985).
35. I. G. DANCE, *Aust. J. Chem.* **31,** 2195 (1978).
36. I. G. DANCE, *J. Chem. Soc. Chem. Commun.* 103 (1976).
37. L.-J. M. MANOJLOVIC, *Nature* **224,** 686 (1969).
38. J. K. MONEY, J. C. HUFFMAN, AND G. CHRISTOU, *Inorg. Chem.* **24,** 3297 (1985).
39. V. M. PADMANABHAN, V. S. YADAVA, Q. Q. NAVARRO, A. GARCIA, L. KARSONO, I-H. SUH, AND L. S. CHIEN, *Acta Crystallogr. Sect. B* **27,** 253 (1971).
40. I. G. DANCE, *J. Am. Chem. Soc.* **102,** 3445 (1980).
41. E. DUBLER AND M. BAUMGARTNER, *Solid State Ionics* **43,** 193 (1990).
42. JCPDS, Powder Diffraction File, Swarthmore, PA.
43. S. DJURLE, *Acta Chem. Sand.* **12,** 1415 (1958).
44. A. PUTNIS, *Philos. Mag.* **34,** 1083 (1976).
45. B. J. SKINNER, *Econ. Geol.* **65,** 724 (1970).
46. A. H. CLARK AND R. H. SILLITOE, *Neues Jahrb. Mineral. Monatsh.* 418 (1971).
47. E. H. ROSEBOOM, *Econ. Geol.* **61,** 641 (1966).